Author/s:
Trenti, M;Padoan, P;Jimenez, R

Title:
THE RELATIVE and ABSOLUTE AGES of OLD GLOBULAR CLUSTERS in the LCDM FRAMEWORK

Date:
2015-08-01

Citation:
Trenti, M., Padoan, P. & Jimenez, R. (2015). THE RELATIVE and ABSOLUTE AGES of OLD GLOBULAR CLUSTERS in the LCDM FRAMEWORK. Astrophysical Journal Letters, 808 (2), https://doi.org/10.1088/2041-8205/808/2/L35.

Persistent Link:
https://hdl.handle.net/11343/118282

DRAFT VERSION JULY 8, 2015
Preprint typeset using LaTeX style emulateapj v. 5/2/11

THE RELATIVE AND ABSOLUTE AGES OF OLD GLOBULAR CLUSTERS IN THE ΛCDM FRAMEWORK

MICHELE TRENTI[1], PAOLO PADOAN[2], RAUL JIMENEZ[2,3]

Draft version July 8, 2015

ABSTRACT

Old Globular Clusters (GCs) in the Milky Way have ages of about 13 Gyr, placing their formation time in the reionization epoch. We propose a novel scenario for the formation of these systems based on the merger of two or more atomic cooling halos at high-redshift ($z > 6$). First generation stars are formed as an intense burst in the center of a minihalo that grows above the threshold for hydrogen cooling (halo mass $M_h \sim 10^8$ M$_\odot$) by undergoing a major merger within its cooling timescale (~ 150 Myr). Subsequent minor mergers and sustained gas infall bring new supply of pristine gas at the halo center, creating conditions that can trigger new episodes of star formation. The dark-matter halo around the GC is then stripped during assembly of the host galaxy halo. Minihalo merging is efficient only in a short redshift window, set by the *ΛCDM* parameters, allowing us to make a strong prediction on the age distribution for old GCs. From cosmological simulations we derive an average merging redshift $\langle z \rangle = 9$ and narrow distribution $\Delta z = 2$, implying average GC age $\langle t_{age} \rangle = 13.0 \pm 0.2$ Gyr including ~ 0.2 Gyr of star formation delay. Qualitatively, our scenario reproduces other general old GC properties (characteristic masses and number of objects, metallicity versus galactocentric radius anticorrelation, radial distribution), but unlike age, these generally depend on details of baryonic physics. In addition to improved age measurements, direct validation of the model at $z \sim 10$ may be within reach of ultradeep gravitationally lensed observations with the *James Webb Space Telescope*.

Subject headings: galaxies: high-redshift — galaxies: general — globular clusters: general — cosmology: theory

1. INTRODUCTION

Globular Clusters (GCs) are compact stellar systems with characteristic mass $\sim 10^5$ M$_\odot$ and radius of a few pc (Heggie & Hut 2003). Their ubiquitous presence around galaxies and their old stellar populations make them tools to investigate early star formation, assembly history of host galaxies, and cosmological models (Katz & Ricotti 2013; Brodie et al. 2014). For example, GC ages were used to constrain the age of the Universe (Jimenez et al. 1996; Krauss & Chaboyer 2003), providing early independent support to the concordance *ΛCDM* model (Planck Collaboration et al. 2013).

Yet, GC formation remains a debated topic with the lack of an established scenario matching all observations. Early proposals identified the high-z Jeans mass ($\approx 10^6$ M$_\odot$) with a protoglobular cloud (Peebles & Dicke 1968). More recently, high-z GC formation as been proposed within dark-matter (DM) halos of mass $M_h \lesssim 10^8$ M$_\odot$, with cooling driven by H_2 (Padoan et al. 1997), as result of shocks induced by a reionization front (Cen 2001), or as purely baryonic systems because stream velocity displaced gas from its parent halo (Naoz & Narayan 2014). Other scenarios focus at somewhat lower redshift, ranging from cooling-induced fragmentation of (proto)-galaxies (Fall & Rees 1985), to formation during galaxy merging/interactions (Ashman & Zepf 1992; Muratov & Gnedin 2010; Li & Gnedin 2014) or within high-density regions of galactic disks (Kravtsov & Gnedin 2005; Kruijssen 2014). Analogies with today's young massive clusters have also been proposed (e.g., Bastian et al. 2013).

The lack of consensus on GC formation may indicate multiple formation mechanisms. In fact, the oldest GCs have essentially uniform ages centered at ~ 12.8 Gyr and spread $\sim 5\%$ (comparable to relative age uncertainty), but wide range of metallicities: from 1% to 1/3 the solar value with high metallicity systems preferentially at small galactocentric radii. In contrast, younger systems show a well defined age-metallicity anti-correlation and higher metallicity at larger galactocentric radii (Forbes & Bridges 2010; Marín-Franch et al. 2009).

In this *Letter* we aim at predicting the probability distribution function of ages for the sub-population of "old" GCs starting from DM halo assembly and merging, which are fully determined (in the statistical sense) by fixing the *ΛCDM* parameters. Our approach parallels studies of evolution of galaxy properties with redshift, such as luminosity/stellar mass functions and clustering, all linked to halo assembly (Trenti et al. 2010b; Lacey et al. 2011; Tacchella et al. 2013; Behroozi et al. 2013).

We propose that old GCs formed via major merging of DM minihalos ($M_{DM} \sim 10^8$ M$_\odot$) that are gas rich (no previous star formation) and metal-enriched through outflows originating from nearby (proto)galaxies. First generation stars form during the merger-triggered burst, while subsequent gas infall through minor mergers can lead to multiple populations. Since the halo merger rate is approximately constant per unit redshift (both for major and minor events; Fakhouri et al. 2010), there is only a short window of opportunity for this mechanism. The redshift needs to be low enough ($z \lesssim 15$) so that minihalos are relatively common, but not too low ($z \gtrsim 6$), otherwise the merger rate drops.

2. GC FORMATION THROUGH MINIHALO-MINIHALO MERGERS

We propose that old GCs form when a host galaxy like the MW is in the earliest stages of its assembly and lacks a well defined disk structure. Its Lagrangian region is still a moderate linear overdensity at $z \sim 10$ containing hundreds of mini-

mtrenti@unimelb.edu.au
[1] School of Physics, The University of Melbourne, VIC 3010, Australia
[2] ICREA & ICC, University of Barcelona, Marti i Franques 1, 08028 Barcelona, Spain
[3] Institute for Applied Computational Science, Harvard University, MA 02138, USA

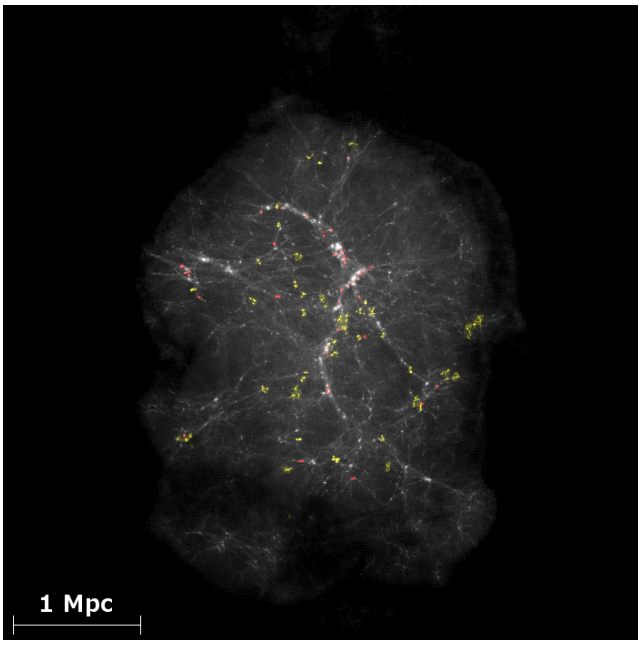

FIG. 1.— Snapshot at $z = 10$ ($t_{lookback} \sim 13.3$ Gyr) of the region that by $z = 0$ will collapse to the halo of mass 8×10^{11} $M_\odot$ shown in the right panels of Figure 4. A linear overdensity containing hundreds of collapsing/collapsed minihalos is present. Regions involved in GC formation through minihalo mergers are highlighed in red (past major merger) and yellow (future merger). A movie capturing redshift evolution is available in the online edition.

halos that are being hierarchically assembled, form stars, pollute their neighbours with metals, and merge to build up a massive system by $z = 0$ (Figure 1).

We assume that compact star clusters form during major mergers of two gas-rich and star-poor minihalos, whose gas has been previously enriched by outflows from nearby halos to $Z \gtrsim 10^{-2}\, Z_\odot$. The combined minihalo mass needs to exceed the threshold for *HI* cooling ($T_{vir} \gtrsim 10^4$ K), but if either of the progenitors was above the cooling mass threshold, it must not have started forming stars yet. Under these conditions, the merger will shock-heat and concentrate the gas, leading to efficient formation of a star cluster. Following the merger-triggered starburst, Type II supernovae clear the gas remaining in the minihalo (escape velocity is a few tens km/s), suppressing further star formation after ~ 10 Myr. Subsequently, slow winds from AGB stars produce chemically enriched gas (D'Ercole et al. 2008), which is retained in the potential well, and diluted by infall of new pristine gas through minor mergers and/or accretion. This gas loading triggers one or more bursts of star formation, more centrally concentrated than the first generation, with merger mass ratios and timing after AGB pollution imprinting diverse chemical signatures in individual clusters, consistent with observations (Renzini 2008). The GC minihalo is eventually incorporated into the merger-tree main branch, with continued mergers and tidal interactions stripping DM and leaving a "naked" GC by $z = 0$. Qualitatively, the scenario is illustrated in Figure 2.

3. QUANTITATIVE MODELING

To evaluate the plausibility of the scenario depicted in Section 2, and compute the GC formation rate, their ages, and spatial distribution at $z = 0$ we resort to a DM-only cosmological simulation run with Gadget2 (Springel 2005), with setup described in Trenti et al. (2009); Trenti & Shull (2010), and Ramirez-Ruiz et al. (2015), but tailored volume/mass resolution and updated cosmology ($\Omega_{\Lambda,0} = 0.685$, $\Omega_{m,0} = 0.315$, $\Omega_{b,0} = 0.0462$, $\sigma_8 = 0.828$, $n_s = 0.9585$, $h = 0.673$; Planck Collaboration et al. 2013). We simulate a 10^3 Mpc^3 (comoving) volume from $z = 150$ to $z = 0$ using $N = 403^3$ particles, while we run a high-resolution version of the same initial conditions to $z = 5.5$ ($t_{lookback} \sim 12.8$ Gyr) with $N = 812^3$ particles (mass resolution 8.3×10^4 $M_\odot$[4]). Our multi-scale approach is based on assigning membership of high-resolution particles to $z = 0$ halos through mapping of particles IDs, and studying halo assembly at higher redshift from the full resolution run, saving snapshots at uniform intervals of 10 Myr.

The high resolution DM-only simulation is post-processed with the star formation and chemical enrichment model of Trenti et al. (2009) to flag minihalos that are in gas-rich, star-free conditions. Specifically, we follow the formation of Population-III (metal-free) stars in halos above the minimum threshold for H_2 cooling with a time-evolving Lyman-Werner background, triggering Population-III star formation when a pristine halo crosses the mass $M_{min}(z)$ shown in Figure 1 of Trenti et al. (2009). Under these conditions, a halo is flagged as enriched by Population-III stars, and then starts forming Population II (metal-enriched) stars once above the hydrogen cooling limit ($T_{vir} > 10^4$ K). As basic description of metal pollution within our DM-only framework, Population-II halos, once they begin forming stars, are assumed to have outflows propagating with spherical symmetry at fixed speed $v_{wind} = 60$ km/s (appropriate for dwarf-like galaxies). Halos that grow with redshift staying below $M_{min}(z)$ until $z \lesssim 13$ (point at which $M_{min}(z)$ corresponds to atomic cooling) may either form a "late-time" Population-III star, or a Population II cluster/dwarf galaxy if polluted by outflows from nearby (proto)galaxies (Trenti & Shull 2010).

As zeroth order characterisation of metal enrichment, we track for each minihalo the number ξ of nearby halos that have metal outflows active for long enough to reach its center. We consider outflow-enriched (pollution counter $\xi \geq 1$), star-free halos with $T_{vir} \sim 10^4$K as potential GC birth-sites. The condition that needs to be satisfied in our framework to create a GC is a major merger with an another smaller outflow-enriched[5] minihalo that increases the mass so that $T_{vir} > 10^4$ K. If either progenitor has $T_{vir} \geq 10^4$K pre-merger, then the merger must happen before stars are formed. Otherwise supernova feedback clears the minihalo of gas. Assuming a typical cooling time of $(1-2) \times 10^8$ yr (Tegmark et al. 1997), we define a timescale $\Delta t = 150$ Myr from crossing of the cooling threshold ($T_{vir} \geq 10^4$K). After such time we no longer consider a GC as the outcome of a major minihalo merger. Furthermore, we define the minimum mass ratio between progenitor halos as $M_2/M_1 > 1/4$.

Finally, we save IDs for all particles involved in GC formation to track halo membership, check for subsequent mergers, and characterize their spatial distribution at $z = 0$ through ID re-mapping into the lower resolution run.

Our simplified gas treatment from DM-only simulations ignores the relative velocity difference between baryons and CDM imprinted at recombination time, which can signifi-

[4] This guarantees that GC minihalos are well resolved with $N \gtrsim 500$ particles, sufficient to characterise their properties (Trenti et al. 2010a).

[5] Mergers between a metal-enriched and a metal-free, star-free minihalo would also satisfy these requirements but such configurations are rare since pairs of merging minihalos have strongly correlated ξ.

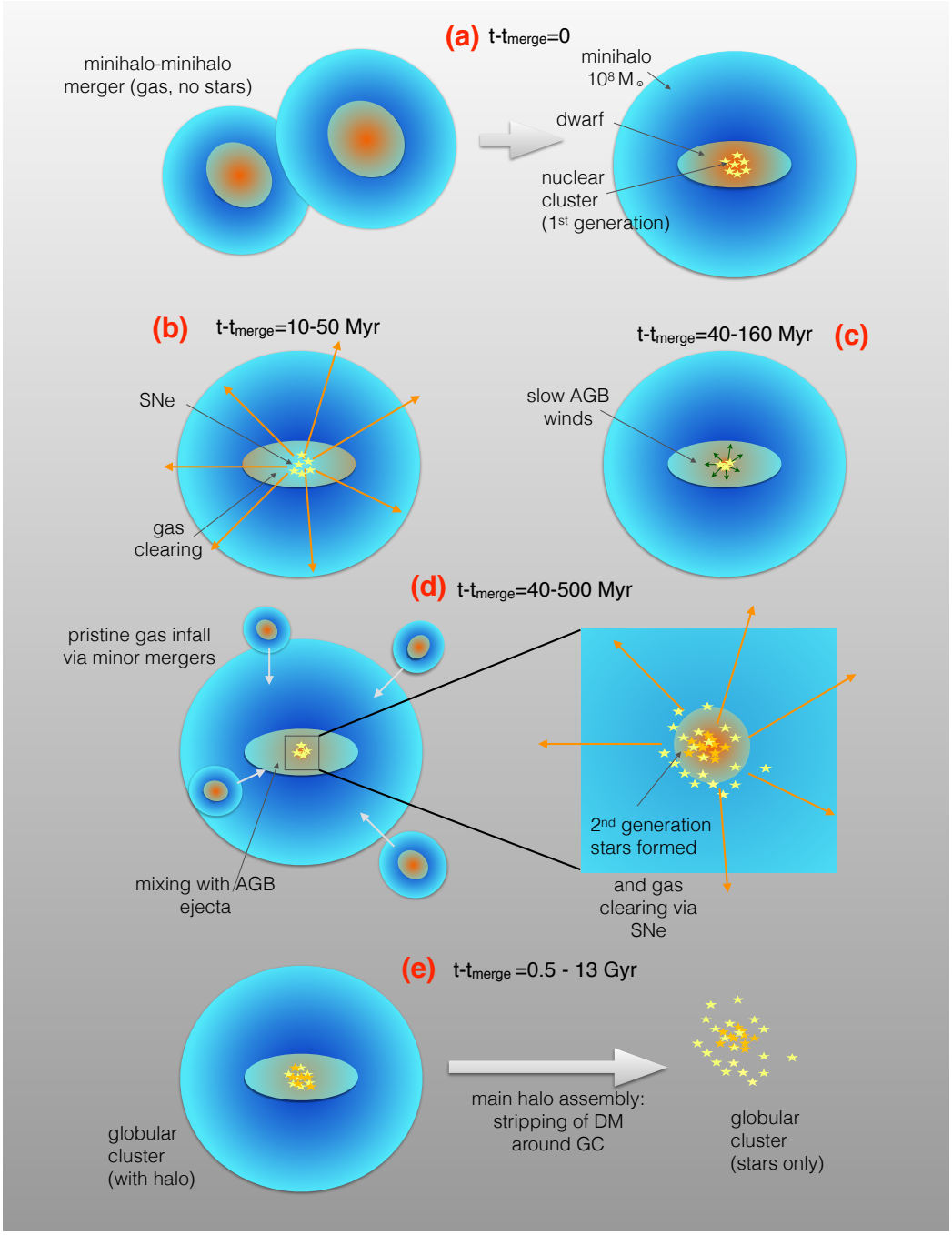

FIG. 2.— Qualitative illustration of GC formation at high-z through a minihalo-minihalo merger (Sec. 2).

cantly impact formation of high-z halos with 10^3 K $\lesssim T_{vir} \lesssim 10^4$ K, suppressing the halo mass function (Tseliakhovich & Hirata 2010; Naoz et al. 2011), and the gas fraction (Naoz et al. 2013). Quantifying the impact of stream velocity for GC formation is difficult without a hydrodynamic simulation, because of competing effects. Gas-rich minihalo mergers require progenitors where Population-III star formation is suppressed. In our framework this happens because of H_2 photodissociation, but stream velocity works as well. In addition, the halo bias would be higher (Tseliakhovich & Hirata 2010), enhancing the merger probability. Overall, the number of gas-rich minihalo mergers may be only moderately suppressed, or possibly even enhanced, in contrast to the $\sim 50\%$ suppression of star formation inferred for the general population of minihalos (Bovy & Dvorkin 2013). We expect our estimate on the GC birth-rate to be accurate within a factor two or better compared to a full treatment of stream velocity.

3.1. *Merger rate and age probability distribution*

Figure 3 shows predictions for the GC formation rate in the most massive simulated halo ($M_h = 4.9 \times 10^{12}$ M$_\odot$, selected for best statistics). At $z > 5.5$ (Universe age < 1 Gyr), there are 279 minihalo-minihalo mergers fulfilling the conditions for GC formation. The average merger redshift is $\langle z \rangle = 9.3$ ($t_{lookback} = 13.2$ Gyr) with dispersion $\Delta z = 1.88$ (age spread ~ 200 Myr). Minihalo-minihalo merging is strongly

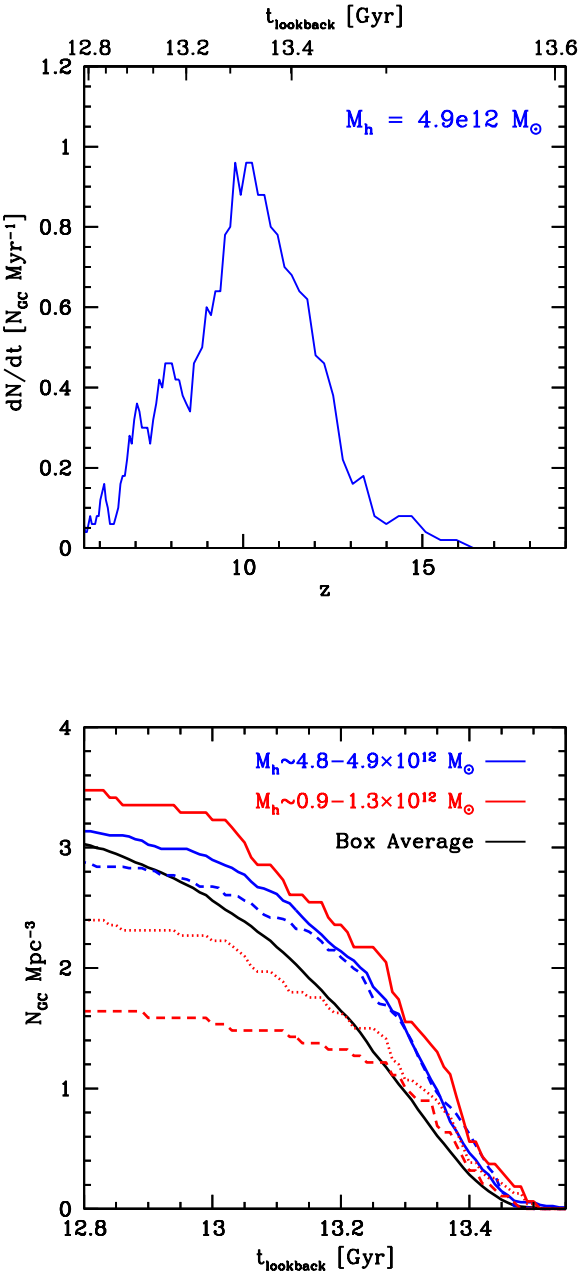

FIG. 3.— Top panel: Formation rate of GCs through minihalo-minihalo mergers in the most massive dark matter halo of our simulation ($M_h = 4.9 \times 10^{12}$ M$_\odot$ at $z = 0$). Data have been smoothed (boxcar filter width 50 Myr). At $z > 5.5$, $N = 279$ clusters are formed with $\langle z \rangle = 9.3$ (dispersion $\Delta z = 1.9$). Bottom panel: Cumulative number of GCs formed per unit volume (Mpc^{-3} comoving) versus lookback time, for the two most massive halos of the simulated volume (solid/dashed blue), for the next three halos in mass ranking (solid, dotted and dashed red), and box-averaged value (black).

peaked with redshift because of competing processes. At $z > 12$ atomic cooling halos are rare, and there is not sufficient time for chemical pollution by outflows originating in nearby star forming sites. Later, as the redshift decreases so does the merger rate (Fakhouri et al. 2010), and at $z \lesssim 8$ structure formation starts shifting toward larger scales. This is qualitatively similar to the circumstances leading to the "Gamov peak" in Nuclear Astrophysics.

Figure 3 is representative of the average GC formation rate, albeit with significant halo-to-halo scatter. Its bottom panel illustrates the cumulative GC number for the five most massive halos in the box comprising a mass range $(0.8-4.9) \times 10^{12}$ M$_\odot$, as well as the box average. The number of GCs is normalised by the comoving volume of each halo in the initial conditions (proportional to halo mass). The box average normalization is the simulation volume. Figure 3 depicts halo-to-halo variations of a factor two. Furthermore, it shows that more massive halos (the five blue and red lines) have slightly older GCs compared to less massive halos (the box average line) by about 100 Myr. This is a consequence of the earlier chemical enrichment and biased halo mass function that is found in overdense environments.

With an average time delay of ~ 250 Myr, the large majority of the products of minihalo-minihalo mergers has a minor merger (progenitor mass ratio $> 1/10$) or receives a mass infall $\geq 10^7$ M$_\odot$ between two snapshots (10 Myr temporal spacing). Major mergers are also frequent: $\sim 25\%$ of the first generation clusters has one. More generally, from Extended Press-Schechter modeling (see Trenti et al. 2008) we derive that a halo with $M_h = 10^8$ M$_\odot$ at $z = 10$ will evolve into a descendant that 500 Myr later (by $z = 5.8$) has doubled in mass at $> 98\%$ confidence. Therefore, the high accretion rate on the minihalos suggests that there is sufficient gas to mix, dilute chemically the AGB ejecta from first generation stars, and concentrate them at the halo center. These conditions can lead to formation of multiple stellar populations (Carretta et al. 2009), widely observed in galactic GCs (Piotto et al. 2007). However, detailed modeling requires hydrodynamic simulations and is beyond the scope of this initial work, focused on making predictions on the robust (parameter-free) probability distribution of GC ages.

Our simulation does not include halos especially representative of the MW/local group because of its small volume. Nevertheless, since minihalo mergers are a universal process, we can rescale the results to estimate the number of old galactic GCs. The MW halo mass is debated, ranging from $\sim 8 \times 10^{11}$ M$_\odot$ to $\sim 4 \times 10^{12}$ M$_\odot$ at 95% (e.g., van der Marel et al. 2012; Phelps et al. 2013; Kafle et al. 2014), almost encompassing the halos shown in Figure 3. In these halos there are 279 to 32 old GCs, suggesting full consistency between observed frequency and predictions in our framework (old GCs in the MW are about 50% of the total population, that is $N \sim 80$). Overall, our theoretical estimate of the old GC number is accurate within a factor two, comparable to halo-to-halo variations. For improved estimates, GC survival to $z = 0$ is also important, as well as detailed modeling of the hydrodynamics (stream velocity, impact of progenitor mass ratio and cooling timescale Δt).

However, all these baryonic processes, including stream velocity, do not affect to first approximation the predicted age distribution, which is the key observable that can falsify our model. In this respect, we note that the GC "formation epoch" shown Figure 3 is that of the minihalo-minihalo merger, and thus an upper limit. Stars form in the following $\sim 10^8$ yr (first generation), and possibly a few hundred Myr later when further gas accretion triggers subsequent generations. Assuming 2×10^8 yr as typical delay for the average stellar age since the merger, our best estimate of the absolute age of old GCs is ~ 13.0 Gyr with a 1σ spread of ~ 0.2 Gyr. This is in full agreement with the current determination of ages for the old GC population $t_{age} = 12.8 \pm 0.6$ Gyr (Marín-Franch et al.

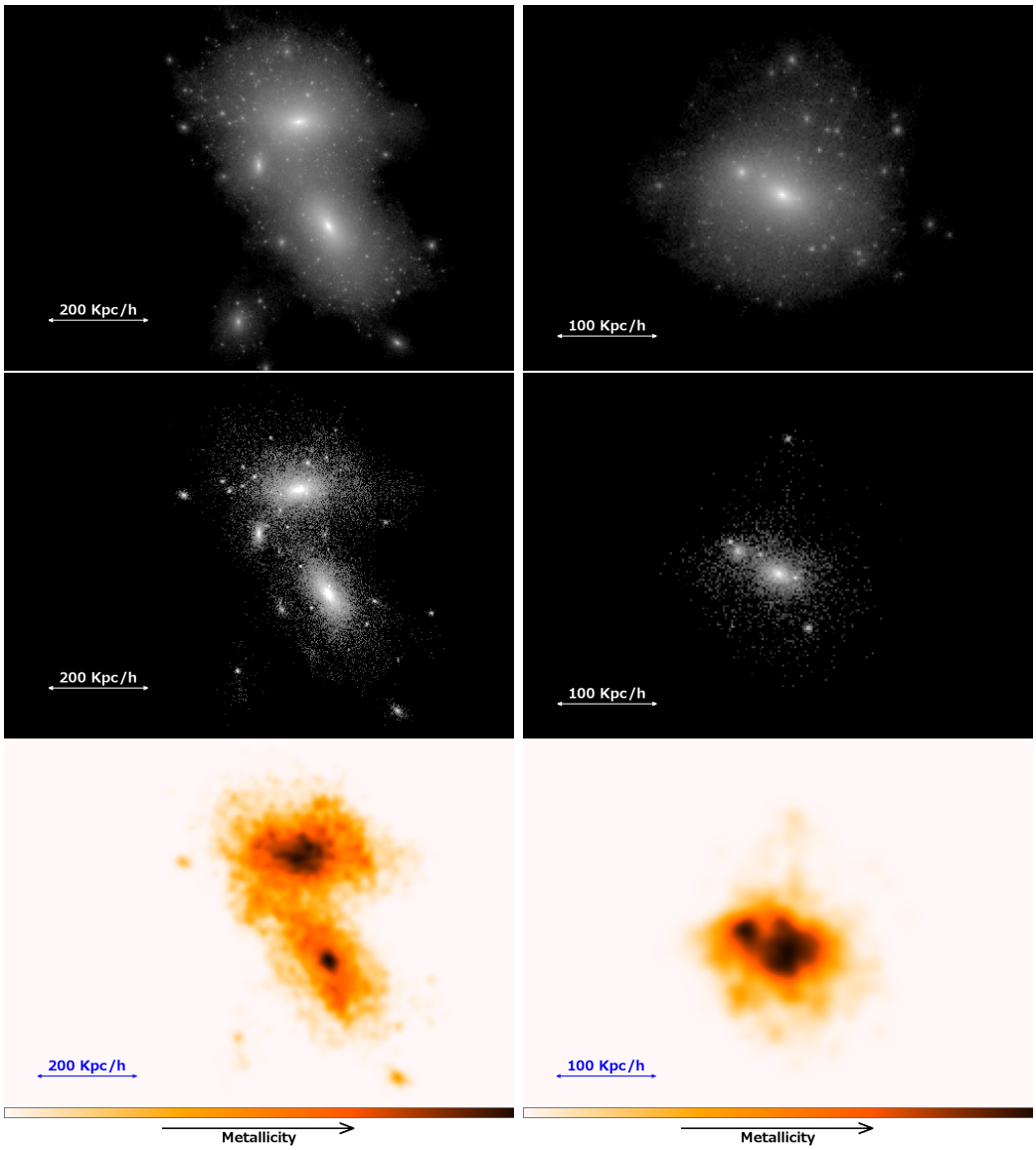

FIG. 4.— Top-left panel: Projected spatial distribution of DM particles in the most massive simulated halo at $z = 0$ ($M_h = 4.9 \times 10^{12}$ M$_\odot$). Bottom-middle panel: Spatial distribution (same redshift and same halo of top-left panel) of the subset of particles that have been part of the $N = 279$ minihalo-minihalo mergers at $z > 5.5$, which we propose are associated to the oldest GCs. Bottom-left panel: Projection of average value of chemical enrichment tag for the total metallicity of GCs (light to dark for increasing number of pollution events), highlighting increasing metallicity at small galactocentric radii in qualitative agreement with observations by Marín-Franch et al. (2009). Right column contains the same panels but for the fifth most massive simulated halo ($M_h \sim 8 \times 10^{11}$ M$_\odot$).

2009). We predict that, if old GCs formed through mini-halo mergers, improvements in absolute and relative age calibrations should converge toward GC formation during the epoch of reionization and age scatter as small as $\Delta t_{age} \sim 0.2$ Gyr.

3.2. *GC masses, galactocentric distribution and tidal stripping*

Our model quantitatively predicts the age distribution of GCs formed through minihalo-mergers, and produces the correct order of magnitude of objects (Section 3.1). To further establish its plausibility, we investigate the expected GC masses, galactocentric distribution and efficiency of tidal stripping in removing DM around GCs by $z = 0$.

A typical star formation efficiency used in studies of high-redshift objects is $\epsilon_* = 0.03$ (stellar to baryonic mass ratio; Alvarez et al. 2012). This gives for a minihalo with $M_h \sim 10^8$ M$_\odot$ a stellar mass $M_* \sim 4 \times 10^5$ M$_\odot$, consistent with the average GC mass $\sim 10^5$ M$_\odot$ (Heggie & Hut 2003), even if there is a diffuse stellar component formed during the merger (and later stripped). Furthermore, our model has a cut-off scale given by the HI cooling mass, naturally predicting a distribution of masses peaked around a characteristic value (log-normal type), as observed for GCs in both the Milky Way and external galaxies (e.g. Harris 1991; Parmentier & Gilmore 2005). Thus, the model has no need to invoke preferential disruption of lower mass star clusters (e.g. Fall & Zhang 2001).

Finally, we discuss model predictions for galactocentric GC distribution and efficiency of tidal stripping of the DM envelope. We tag in the $z = 0$ snapshot the particles associated to GC formation in the high-resolution, high-z run. Results are shown in Figure 4: tagged particles (middle panel) have

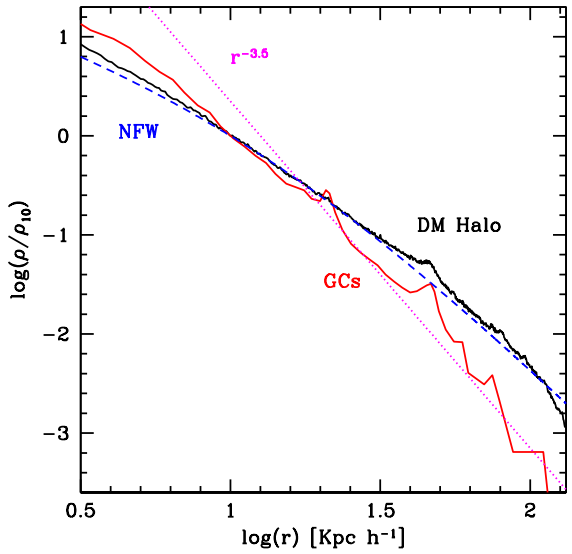

FIG. 5.— Density profile versus galactocentric radius at $z = 0$ for the halo shown in the right panels of Figure 4. The DM density (black-solid line) is well represented by a NFW profile (dashed-blue line), while particles associated to minihalo-minihalo mergers have a steeper profile (solid red), consistent with $\rho \sim r^{-3.5}$ observed in the distribution of Galactic GCs (dotted magenta). Profiles have been normalized at $r = 10$ Kpc h^{-1}.

higher galactocentric concentration compared to all particles (top panel). The $z = 0$ radial density profile of GC particles is shown in Figure 5 for a typical non-interacting halo, demonstrating that it follows the slope $\rho(r) \sim r^{-3.5}$ observed in the distribution of MW GCs. This is not surprising since minihalo mergers are $\gtrsim 2\ \sigma$ DM peaks at $z \sim 9$, which Moore et al. (2006) found to be distributed with a $\rho(r) \sim r^{-3.5}$ profile by $z = 0$. The middle panels of figure 4 also show a diffuse distribution of particles involved in minihalo mergers. This supports our proposal that tidal interactions during the merger process strip GCs of their initial DM halos, although the results need to be confirmed by a full high-resolution simulation to $z = 0$. Last, through particle tagging we derive the correlation between $z = 0$ galactocentric distance and chemical enrichment (Fig. 4, bottom panels). As observed by Marín-Franch et al. (2009), we qualitatively obtain a negative correlation between galactocentric radius and metallicity, with GCs located centrally enriched by up to $\xi = 15$ polluters, and those in the outskirts having $\xi = 1-2$.

4. CONCLUSIONS

The observed age-metallicity distribution of galactic GCs shows a bimodal population, with about half the objects residing along an "old" branch with age $\sim 12.8 \pm 0.6$ Gyr and spread comparable to the relative age error (Marín-Franch et al. 2009; Forbes & Bridges 2010). Here, we explored a novel idea to form these old GCs at the center of DM minihalos with virial temperature $T_{vir} \gtrsim 10^4$ K ($M_h \sim 10^8$ M$_\odot$) and with the following additional constraints:

- Enrichment by metal outflows from nearby Population-II halos rather than by their own Population-III star formation;
- Major merger with a similar metal-enriched, but star-free minihalo within a time $\Delta t \sim 150$ Myr from the crossing of the cooling threshold ($T_{vir} \gtrsim 10^4$ K).

The minihalo-minihalo merger is the key new ingredient to create a compact star cluster. While the details of star formation depend on complex baryonic physics that will be explored in future investigations, we make robust and falsifiable predictions on the probability distribution of the minihalo mergers (age of GCs), which are discussed in Section 3.1. We obtain $\langle t_{age} \rangle = 13.0$ Gyr and $\Delta t_{age} \sim 0.2$ Gyr, in agreement with current observations.

Improvements in GC age measurements can uncontroversially falsify the minihalo merger scenario. Also, model predictions may be within reach of direct observations with the *James Webb Space Telescope* (JWST). In fact, the number density of compact star clusters at $z > 7$ is sufficiently high (1.5×10^4 arcmin^{-2}) that JWST can identify some of them if highly magnified ($\mu \sim 100$) to $M_{AB} \sim -17$ by a foreground galaxy cluster. However, we note that it will be challenging to discriminate against other compact high-z objects such as Population-III clusters (e.g., Zackrisson et al. 2012).

Besides GC ages, other aspects of the framework such as multiple stellar populations formation triggered by minor mergers (Section 2) are more speculative, since they depend on a complex interplay between baryonic and DM physics. We presented consistency checks in Section 3.2 to characterize qualitatively the distribution of GCs, their metallicity and stripping of the DM halo envelope, but further work is required. In addition to detailed investigation of DM stripping, perhaps one interesting aspect to follow-up is the connection between GCs and dwarf galaxies. While earlier studies considered them as two distinct classes in the luminosity-size plane, recent work unveiled the existence of ultracompact dwarf galaxies with intermediate properties (e.g., Jennings et al. 2014). Indeed, our framework predicts a continuum between classical dwarf galaxies (no major mergers at formation, DM dominated) and old GCs (major merger, DM envelope stripped by $z = 0$). Overall, minihalo mergers appear to provide a promising scenario to explore for the formation of the oldest GCs observed in today's galaxies.

It is our pleasure to thank Duncan Forbes, Diederik Kruijssen and Sasha Muratov for useful discussions on an earlier version of the manuscript, and an anonymous referee for helpful comments.

REFERENCES

Alvarez, M.A., Finlator, K., & Trenti, M. 2012, ApJ, 759, L38
Ashman, K.M., & Zepf, S.E. 1992, ApJ, 384, 50
Bastian, N., Lamers, H.J.G.L.M., de Mink, S.E., et al. 2013, MNRAS, 436, 2398
Behroozi, P.S., Wechsler, R.H., & Conroy, C. 2013, ApJ, 770, 57
Bovy, J. and Dvorkin, C. 2013, ApJ, 768, 70
Brodie, J.P., Romanowsky, A.J., Strader, J., et al. 2014, ApJ, 796, 52
Carretta, E., Bragaglia, A., Gratton, R.G., et al. 2009, A&A, 505, 117
Cen, R. 2001, ApJ, 560, 592
D'Ercole, A., Vesperini, E., D'Antona, F., McMillan, S.L.W., & Recchi, S. 2008, MNRAS, 391, 825
Fakhouri, O., Ma, C.P., & Boylan-Kolchin, M. 2010, MNRAS, 406, 2267
Fall, S.M., & Rees, M.J. 1985, ApJ, 298, 18
Fall, S.M., & Zhang, Q. 2001, ApJ, 561, 751
Forbes, D.A., & Bridges, T. 2010, MNRAS, 404, 1203
Harris, W.E. 1991, ARA&A, 29, 543

Heggie, D., & Hut, P. 2003, Cambridge University Press
Jennings, Z.G., Strader, J., Romanowsky, A.J., et al. 2014, AJ, 148, 32
Jimenez, R., Thejll, P., Jorgensen, U.G., MacDonald, J., & Pagel, B. 1996, MNRAS, 282, 926
Kafle, P.R., Sharma, S., Lewis, G.F., & Bland-Hawthorn, J. 2014, ApJ, 794, 59
Katz, H. and Ricotti, M. 2013, MNRAS, 432, 3250
Krauss, L.M., & Chaboyer, B. 2003, Science, 299, 65
Kravtsov, A.V., & Gnedin, O.Y. 2005, ApJ, 623, 650
Kruijssen, J.M.D. 2014, ArXiv e-prints, arXiv:1407.2953
Lacey, C.G., Baugh, C.M., Frenk, C.S., & Benson, A.J. 2011, MNRAS, 412, 1828
Li, H. and Gnedin O.Y. 2014, ApJ, 796, L10
Marín-Franch, A., Aparicio, A., Piotto, G., et al. 2009, ApJ, 694, 1498
Moore, B., Diemand, J., Madau, P., Zemp, M., & Stadel, J. 2006, MNRAS, 368, 563
Muratov, A. and Gnedin, O.Y. 2010, ApJ, 718, 1266
Naoz, S., & Narayan, R. 2014, ApJ, 791, L8
Naoz, S., Yoshida, N. and Barkana, R. 2011, MNRAS, 416, 232
Naoz, S., Yoshida, N. and Gnedin, N.Y. 2013, ApJ, 763, 27
Padoan, P., Jimenez, R., & Jones, B. 1997, MNRAS, 285, 711
Parmentier, G., & Gilmore, G. 2005, MNRAS, 363, 326
Peebles, P.J.E., & Dicke, R.H. 1968, ApJ, 154, 891
Phelps, S., Nusser, A., & Desjacques, V. 2013, ApJ, 775, 102
Piotto, G., Bedin, L.R., Anderson, J., et al. 2007, ApJ, 661, L53
Planck Collaboration, Ade, P.A.R., Aghanim, N., et al. 2013, arXiv:1303.5076
Ramirez-Ruiz, E., Trenti, M., MacLeod, M. et al. 2015, ApJ, 802, L22
Renzini, A. 2008, MNRAS, 391, 354
Springel, V. 2005, MNRAS, 364, 1105
Stiavelli, M., & Trenti, M. 2010, ApJ, 716, L190
Tacchella, S., Trenti, M., & Carollo, C.M. 2013, ApJ, 768, L37
Tegmark, M., Silk, J., Rees, M.J., et al. 1997, ApJ, 474, 1
Trenti, M., Santos, M.R., & Stiavelli, M. 2008, ApJ, 687, 1
Trenti, M., & Shull, J.M. 2010, ApJ, 712, 435
Trenti, M., Smith, B.D., Hallman, E.J., Skillman, S.W., & Shull, J.M. 2010a, ApJ, 711, 1198
Trenti, M., Stiavelli, M., Bouwens, R.J., et al. 2010b, ApJ, 714, L202
Trenti, M., Stiavelli, M., & Shull, J.M. 2009, ApJ, 700, 1672
Tseliakhovich, D. and Hirata, C. 2010, PRD, 82, 083520
van der Marel, R.P., Fardal, M., Besla, G., et al. 2012, ApJ, 753, 8
Zackrisson, E., Zitrin, A., Trenti, M., et al. 2012, MNRAS, 427, 2212